Astrocyte spreading and migration on aggrecan–laminin dot gradients

Tony W. Hsiao, Patrick A. Tresco, and Vladimir Hlady[a)]
Department of Bioengineering, University of Utah Salt Lake City, Utah 84112, USA

(Received 3 May 2017; accepted 17 July 2017; published 11 September 2017)

The surface concentration gradient of two extracellular matrix (ECM) macromolecules was developed to study the migratory and morphological responses of astrocytes to molecular cues typically found in the central nervous system injury environment. The gradient, prepared using microcontact printing, was composed of randomly positioned micrometer-sized dots of aggrecan (AGG) printed on a substrate uniformly coated with laminin (LN). AGG dots were printed in an increasing number along the 1000 μm long and 50 μm wide gradient area which had on each end either a full surface coverage of AGG or LN. Each dot gradient was surrounded by a 100 μm-wide uniform field of AGG printed over laminin. Seeded astrocytes were found to predominantly attach to LN regions on the gradient. Cellular extensions of these cells were longer than the similar processes for cells seeded on uniform substrates of AGG or LN serving as controls. Astrocyte extensions were the largest and spanned a distance of 150 μm when the cells were attached to the mixed AGG+LN patches on the gradient. As evidenced by their increased area and perimeter, the cells extended processes in a stellate fashion upon initial attachment and maintained extensions when seeded in AGG+LN regions but not on uniform laminin controls. The cells migrated short distances, ~20–35 μm, over 24 h and in doing so preferentially shifted from AGG areas to higher LN surface coverage regions. The results indicated that presenting mixed ECM cues caused astrocytes to sample larger areas of the substrate and made the cells to preferentially relocate to a more permissive ECM region. © *2017 American Vacuum Society*. [http://dx.doi.org/10.1116/1.5001675]

I. INTRODUCTION

After central nervous system (CNS) injury, resident astrocytes serve important functions to reduce damage by restoring homeostasis, sequestering invading cells, and preserving neuronal cells.[1–3] Astrocytes are also responsible for the neuron inhibitory extracellular matrix (ECM) rich in chondroitin sulfate proteoglycan (CSPG) that is produced following CNS injury.[4] These contrasting characteristics largely arise due to the heterogeneous nature of astrocytes and the varying time course of their roles as the neuroprotective impacts are overshadowed by CSPG production over the course of injury healing.[2,5] The ability of astrocytes to migrate in the recovering CNS environment over compact lesions has been shown to be beneficial for functional recovery.[6]

Several approaches have been undertaken to understand how astrocytes migrate both *in vivo* and *in vitro*. Xenogenic astrocyte transplants into mice showed that astrocytes migrated at a rate of 220 μm/day before slowing.[7] Transplanted astrocytes from primary cultures actively entered multiple regions of brain tissue.[8,9] In contrast, there was no marked migration of cortical astrocytes after stab wounds.[10] This lack of migration has also been observed in real time: after traumatic brain injury, live tracking of astrocytes showed that there was no bulk recruitment or migration of astrocytes to the wound site, but rather an increase in proliferation of cells adjacent to the injury.[11] However, a subset of astrocytes from the proliferative subventricular zone were shown to migrate to the ischemic cortex and have neuroprotective functions.[12] *In vitro*, scratch wound assays have been commonly used to investigate how astrocytes close gaps in confluent monolayers. Astrocytes at the edge proliferate, but individual cells show limited movement.[13] They also upregulate ECM molecule production, especially laminin (LN) and CSPG.[14,15] This behavior leads to eventual closing of the defect.

There is conflicting evidence regarding the role of astrocytes in the injury site. Astrocytes placed in collagen scaffolds and differentiated with bone morphogenetic protein aided functional recovery after spinal cord injury in rats.[16] Conversely, the application of collagen fiber-based scaffolds that also improved functional outcomes in canines showed that grafts were not heavily populated with astrocytes, while neurons continued to be able to grow.[17] In contrast, polylactic acid microfibers were shown to concurrently direct both astrocyte and neuronal growth when used to bridge a spinal transection.[18] While it is unclear if populating scaffolds with astrocytes are important for functional recovery, *in vitro* studies have shown that aligned astrocytes increase outgrowth and convey directionality to neurons themselves.[19,20] Alignment of astrocytes and a subsequent decrease in reactivity can be accomplished using electric fields, topographical features, and molecular cues.[20–24]

Rather than a uniform coating of chemoattractants, a potential stimulus for guiding astrocytes onto scaffold surfaces could include a directional gradient containing substrate-bound attractive and/or repulsive molecular cues. Such surface gradients have been valuable in studying neuronal behavior,[25–29] which can be missed in the absence of subtle concentration changes of molecular cues.[30] Laminin has been shown to be

[a)]Author to whom correspondence should be addressed; present address: 20 S. 2030E., Rm. 108A, Salt Lake City, UT 84112; electronic mail: vladimir.hlady@utah.edu

supportive of astrocyte adhesion and migration,[15] while aggrecan (AGG), a proteoglycan with CSPG chains, was often selected as a model inhibitory component. Aggrecan is produced by astrocytes and is known to inhibit Schwann cell migration.[31] Aggrecan has also been shown to have a limited alignment effect on astrocytes.[32]

In the present study, we designed gradient stripes of randomly placed micrometer-size aggrecan dots attached to a uniform film of laminin and used time-lapse microscopy to observe the migration of astrocytes after seeding. Microcontact printing was used to print AGG surface dots in an increasing number along the 50 μm wide and 1 mm long stripe that was surrounded by a 100 μm-wide uniform field of AGG printed over laminin (Fig. 1). In this substrate design, each gradient lane of aggrecan also contained a countergradient of laminin. Random placement of aggrecan patches in gradients resulted in a lack of periodicity typically found in alternative surface pattern designs.[28,29,33,34] Astrocyte migratory and morphological responses to the aggrecan–laminin countergradient and their preference for one or the other molecular cues were measured over 24 h and quantified.

II. MATERIALS AND METHODS

A. Cell culture

Primary P1-3 astrocytes were harvested from Sprague-Dawley rats according to an established protocol.[35] Cortical astrocytes were cultured for one week, shaken to remove other cell types, and then frozen in liquid nitrogen prior to use. Cells were thawed and cultured for 1–2 weeks in Dulbecco's modified Eagle's medium/F12 media (Gibco) supplemented with 10% fetal bovine serum (Atlanta Biologicals) prior to treatment with 0.25% trypsin and placement onto gradient patterns. Astrocytes were seeded at a low density of 5000–6000 cells per square centimeter in SATO^{-} serum-free medium.[36] Astrocytes were cultured at 5% CO_2 and 37 °C for the duration of the experiments. Only astrocytes which were visibly attached to the surfaces were imaged for subsequent analyses.

B. Gradient surface patterning

Dot gradients were designed using Mathematica (Wolfram) to randomly place pixels as previously described.[37] The gradients were 1000 μm long and 50 μm wide and spaced 100 μm apart by a region of full AGG surface coverage to separate gradient stripes with large areas of uniformly stamped molecular cue and prevent conflicting gradient interactions. The design was then translated using L-Edit (Tanner) to create a file for an electromask pattern generator to expose onto a photoresist-coated mask (Telic). Polydimethylsiloxane was cast on the mask to form a stamp for microcontact printing. To visualize the stamped protein gradient, AGG (A1960, Sigma) was fluorescently labeled with Alexa Fluor 594 (A-20004, Invitrogen) and eluted through a PD-10 Sephadex column (GE Healthcare) with phosphate buffered saline (PBS) to remove unreacted fluorophore. The AGG solution was diluted to a concentration of 0.3 mg/mL in PBS and stored at 4 °C until use. Glass-bottomed petri dishes (Fluorodish) were first coated by adsorption of LN (L2020, Sigma-Aldrich) from a 0.3 mg/mL solution at 4 °C overnight, then rinsed with double-distilled, deionized water (DDI), and dried under nitrogen prior to microcontact printing. Gradient stamps were adsorbed with labeled AGG solution for 1–2 h at room temperature, then rinsed thrice with DDI, and dried with nitrogen. Stamps were manually placed into conformal contact with the glass dish bottoms and remained in contact for 5–10 min prior to stamp removal. Gradient transfers were confirmed by imaging the fluorescently labeled protein.

C. Time-lapse microscopy

A fully automated Olympus IX81 inverted microscope with a 20× objective was used to image astrocytes in glass-bottomed dishes. A custom-machined aluminum holder was

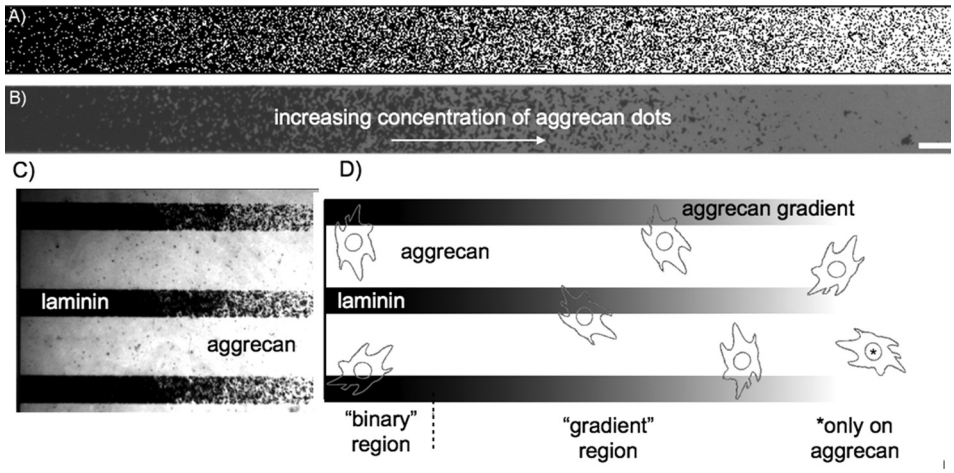

FIG. 1. Dot gradient pattern transfer and definitions of different regions. (a) Computer-generated dot gradient template and subsequently fabricated polymeric stamp led to (b) transferred fluorescent pattern onto glass. Scale bar = 25 μm. (c) Schematic of astrocyte characterization based on interaction with gradient patterns. Astrocytes in binary footprint regions did not encounter micrometer-sized patterns. Cells which encountered only aggrecan were grouped in analysis with astrocytes cultured on uniform aggrecan controls. Representative images of astrocytes interacting with the AGG/LN gradient and binary footprint regions are shown in panel (d).

used to securely keep dishes in the temperature-controlled stage chamber. Uncovered dishes filled with DDI water were included in the chamber to maintain humidity. Metamorph imaging software (Molecular Devices) was used to control the computerized stage, filters, and CCD camera to automatically take images every 5 min for chosen locations. The built-in autofocus function of the software was used for every five images over the imaging period. The captured digital images were mapped to 0.65 μm per pixel. For substrates with AGG+LN gradients, cells were allowed to attach for 4 h postseeding and then were imaged for 20 h. A substrate with a uniform adsorbed laminin coating was used as a control. On this substrate, the cells were imaged within 30 min postseeding for 24 h. Areas with cells that left the field of view, underwent apoptosis, or were obscured by debris or intercellular contact were neglected. All images had background correction using a fitted 2D cubic polynomial prior to analysis.

D. Astrocyte morphology quantification

Astrocyte outlines were measured for each cell with the aid of the ESnake plugin for IMAGEJ (NIH).[38] The ESnake setting for control points ranged from 20 to 50 based on cell size and morphology complexity. The Gaussian blur setting was adjusted from 2 to 8 depending on image contrast. Cell images taken every 30 min were analyzed. Cell outlines were measured using ImageJ to quantify the perimeter, area, centroid, circularity (4π*area/perimeter^2), and maximum span (Feret diameter). The cell centroid was subsequently used to calculate the speed of migration and overall cell displacement. To analyze the changes in astrocyte migratory and morphological behaviors, measurements from the first (4 h postseeding) and last (24 h postseeding) observations were compared and reported as *initial* and *final* parameters, respectively.

Astrocytes were divided into three categories based on the composition of the underlying substrate. For controls, the cells were cultured on uniform adsorbed LN (n = 15) or AGG stamped over LN (n = 6) substrates. Astrocytes that attached with some portion of their cell body to the AGG+LN gradient area over the culture period were identified as *gradient* cells (n = 8). Cells that attached on the extreme end of the gradient where there were no printed AGG dots were presented with a *binary* choice of substrates: a 50 μm wide stripe of 100% coverage of laminin or 100% coverage of aggrecan in the neighboring areas. Such cells were classified as *binary* footprint cells (n = 6). The length of the binary regions varied slightly with each sample but typically covered around the first 100 μm of the stamped gradient pattern. Data were tested for statistical significance using an analysis of variance with a Tukey-honest significant difference posthoc test ($\alpha = 0.05$).

E. Assessment of protein preference

To determine how astrocytes migrate and shift their locations with respect to the underlying AGG+LN pattern, the fluorescence intensities of the areas underneath the cells with printed AGG (Alexa Fluor 594 labeled) and adsorbed LN (unlabeled) patterns were compiled into fluorescence intensity histograms. For example, an area below the cell attached only to LN would have a single low fluorescence intensity peak, while a cell attached to AGG would cover the area of a single high fluorescence intensity peak. Cells attached to the mixed AGG+LN patches would have a fluorescence intensity distribution, showing both fluorescence intensities with different peak heights corresponding to their actual position. When the cell migrated over time, the magnitudes of low and high intensity peaks changed as the substrate coverage of AGG and LN patches covered by the cell changed. Only the cells in mixed AGG+LN gradient regions (i.e., cells with histograms that displayed these two distinct fluorescence intensity peaks) were used for analysis (n = 7). The heights of the two histogram peaks were measured at 5 h intervals to track changes in the substrate composition below individual astrocytes over time.

III. RESULTS

A. Dot gradient stamps successfully transferred AGG+LN gradients to glass substrates

AGG+LN dot gradients were successfully transferred to glass using microcontact printing methods. The printed dot size was altered both by random distribution of the dots and by the coalescence of neighboring small surface features. After the transfer of AGG+LN dot gradients to glass substrates, their imaging revealed that small stamp features, like isolated dots or voids, were often lost compared to the original template [Figs. 1(a) and 1(b)]. This made the printed gradient steeper than originally designed and also resulted in areas near each end of the gradient with uniform surface coverages of LN or AGG [Fig. 1(c)]. Astrocytes that never encountered LN (i.e., attached to the uniform AGG ends or areas between the gradient stripes) were grouped with cells cultured on the uniform AGG control substrate for the purpose of morphological analysis. Cells which encountered the mixed AGG+LN patches along the gradient were classified as *gradient* cells. The third category included *binary* cells; astrocytes not only interfaced with the uniform LN end of the gradient but also partially adhered to the AGG area surrounding that gradient end [Fig. 1(d)].

B. Astrocytes exhibit the stellate morphology during early attachment on LN

During initial attachment within 30 min of seeding on control LN substrates with uniform adsorbed laminin, astrocytes first extended long processes followed by retraction and spreading of the cell body (Fig. 2). Due to the latency required to determine astrocyte locations on gradient patterns, this early spreading behavior could not be observed on gradients. On control AGG substrates, however, cells maintained more active processes over the entire culture time (Fig. 3).

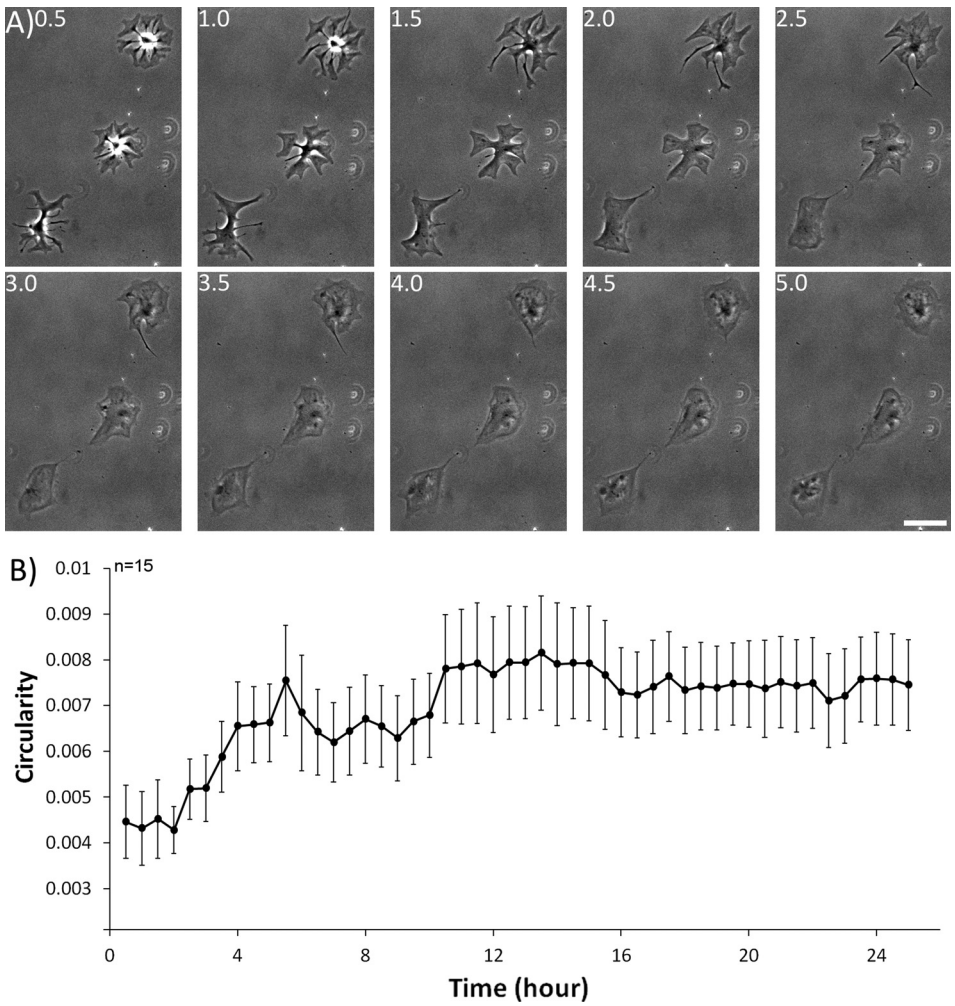

FIG. 2. Initial stellate spreading of astrocytes on the uniform LN coated substrate is observed prior to the final amoeboid morphology. (a) Representative image of three astrocytes during the initial 5 h attachment period. Scale bar = 50 μm. (b) Circularity of astrocytes on control LN substrates measured over time indicated that a period of 5 h was required to achieve a stable, round morphology. Error bars indicate ±standard error of the mean (SEM).

C. Mixed AGG+LN dot areas caused astrocytes to increase the process extension length

Astrocytes on uniform laminin substrates were more evenly amoeboid than cells on the other types of substrates and attained the smallest average perimeters while having similar cell areas. Average cell perimeters on LN remained unchanged between initial and final time points. Similarly, astrocyte footprint areas on the LN substrate were little changed [Figs. 4(a) and 4(b)]. Astrocytes had similar sizes on uniform AGG versus on mixed AGG+LN areas both at initial and final observations, but cells on these two substrates doubled in size over the course of the experiment.

The presence of micrometer-sized patches of AGG in the gradients caused the astrocytes to extend processes such that the perimeter of these cells was higher than on any other surface type at both the initial and final time points. In addition, the cells on mixed AGG+LN areas also had a significant 25% increase in the average perimeter over the time of the study while maintaining a significantly less circular morphology compared to cells on control LN substrates [Fig. 4(c)]. Astrocytes in AGG and binary regions had similar perimeters which were smaller than those for gradients but were approximately 30% larger than those on uniform LN controls at the final time point. Astrocytes on substrates other than LN were less amoeboid in general. Astrocytes appeared to attach to micrometer-sized patches of LN, and some astrocytes at the binary footprint location extended along the 5 μm wide gap of LN between gradient patterns.

Astrocyte spreading resulted in an average span of around 65 μm after initial attachment on all substrates [Fig. 4(d)]. However, over the next 20 h, astrocyte spans on uniform LN controls remained largely unchanged, while astrocytes on uniform AGG had a significant increase in span over that time. Astrocytes attached on gradient areas and binary locations had an even larger increase in maximum span to an average of around 150 μm but were not significantly different from each other. Both pattern types ("gradient" and "binary") caused astrocytes to have a span nearly double that of cells on uniform LN substrates. The span for an individual cell ranged from 40 μm at the smallest and 220 μm at the largest across all samples.

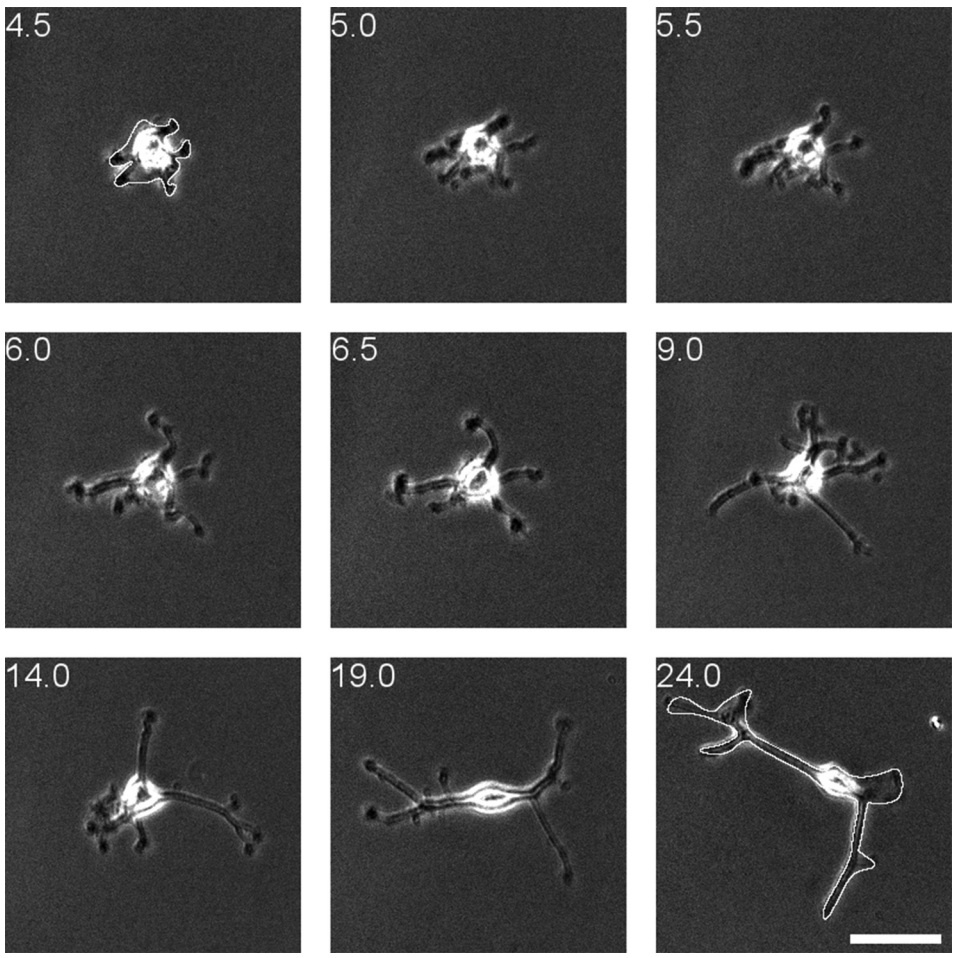

FIG. 3. Astrocyte spreading on the aggrecan surface. The progression of an astrocyte spreading on aggrecan at 0.5 h intervals. Measured outlines are shown for the 4.5 and 24.0 h time points only. Scale bar = 50 μm.

D. Astrocyte migration speed was largely unchanged on types of substrates

Astrocytes migrated at an average speed of around 10 μm/h on all substrate types [Fig. 4(e)]. There were no discernible differences between astrocytes' migration speeds at initial and final observations. Among all observations, astrocyte speed ranged from less than 1 to up to 120 μm/h. There was also no significant difference in overall displacement over time of cell culture between different substrates, with cells being located on average 20–35 μm away from their initial locations [Fig. 4(f)]. Distances covered by individual astrocytes ranged from 1 to over 65 μm.

E. Astrocytes preferred LN over AGG substrates

When the fluorescence intensity below each cell was presented in a form of a histogram [Fig. 5(a), inset], the magnitude of the higher fluorescence intensity peaks (AGG area) was found to decrease over culture time, while the low fluorescence intensity peak (LN area) showed an opposite trend [Fig. 5(a)]. These changes in the substrate composition below the attached cells illustrate how the cells that encountered both AGG and LN patches at some point preferentially moved their cell bodies onto LN areas by the end of the observation period [Fig. 5(b)]. This behavior consisted of an initial preference of cellular extensions toward LN followed by an eventual shift of the cell body. Astrocytes which initially encountered no LN patches extended the process in all directions until LN was contacted, and then, preferential extension and shifting occurred toward LN at later time points.

IV. DISCUSSION

A. Astrocytes extend processes not seen on uniform, adhesive culture substrates

While the alignment of astrocytes on substrates patterned with ECM molecules has been well documented,[20,22] much less is known about how astrocytes interact with substrates containing composite permissive and inhibitory ECM molecular cues. One rationale for deciphering responses of astrocytes to such complex environments is to find whether there is a causal relationship between the presented molecular cues and the astrocyte morphology and migration. Although the astrocyte morphology cannot be used as a direct indicator of their reactivity, especially at the CNS injury site,[5] it is interesting to note that astrocytes on standard culture substrates, such as tissue-culture polystyrene, poly-L-lysine, or

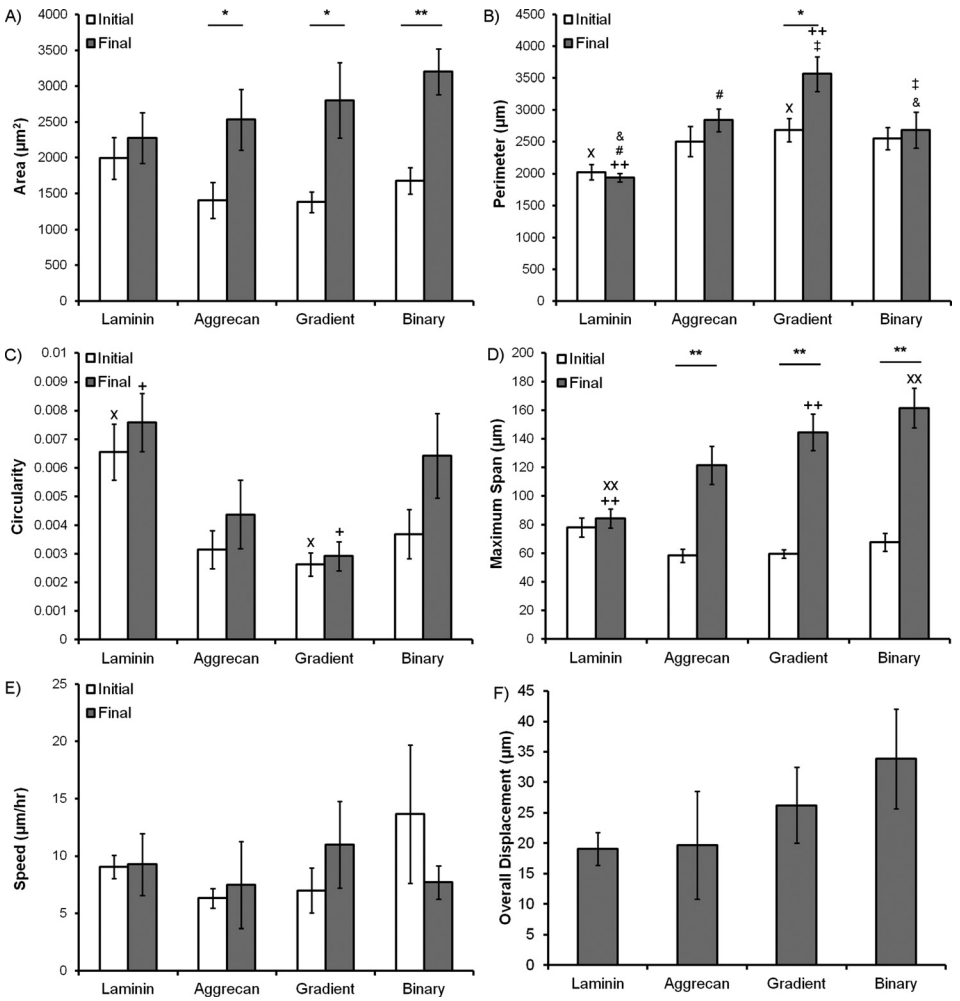

FIG. 4. Average astrocyte morphology parameters on various substrates. (a) Area, (b) perimeter, and (c) circularity of cells at initial and final observations. (d) Maximum span, (e) speed, and (f) overall displacement from the initial attachment location for astrocytes on the given pattern regions and uniform surfaces. Statistically significant differences over time are indicated (*$p < 0.05$; **$p < 0.005$) and significant differences between substrates are indicated by matching symbols (x, +, ‡, & = $p<0.05$; xx, ++ = $p<0.005$). Error bars indicate ±SEM.

laminin, exhibit a more amoeboid morphology than the stellate shape observed in the CNS. The observation of the initial spreading of astrocytes in a stellate fashion (Fig. 2) indicated that the presence of the uniformly adhesive substrate caused astrocytes to change their shape over the course of several hours. Astrocytes presented with the composite micrometer-sized patches of AGG and LN showed the greatest extent of process extension as evidenced by their large perimeters (Fig. 4). Although altering the morphology of astrocytes from amoeboid to stellate on topographically organized substrates has been show to decrease several markers of astrocyte reactivity,[23,24] it remains uncertain which receptors are involved and by which intracellular signaling in regulating astrocyte reactivity takes place. Blocking individual receptors and/or assessing the glial fibrillary acidic protein and CSPG expression of the more stellate astrocytes, observed here at only early time points, could provide further insight into the relationship between the morphology and reactivity. Such experiments could lead to substrate patterns that would be more effective at reducing astrocyte reactivity and generating less reactive and more quiescent astrocyte cultures, such as with 3D gels and various alternative ECM substrates.[39,40]

B. Astrocytes are capable of sampling between large distances

The present measurements indicate that astrocytes were able to sample immobilized ECM molecules separated by as large as 150 μm. The greatest extensions for these cells were triggered by the presence of mixed molecular cues within the AGG+LN gradient. When presented with mixed substrate choices for attachment, the cell extended processes farther as a means to "find" a more suitable ECM component for its final location. In the case of a less preferable substrate like AGG, the spans and perimeters of astrocytes were higher than those of LN, indication of an attempt to find more permissive attachment areas (Figs. 3 and 4). It is also possible that this difference in behavior was due to a subset of cells that were more prone to adhesion onto AGG and therefore were also more likely to extend processes and avoid ameboid spreading. However, astrocytes on LN also

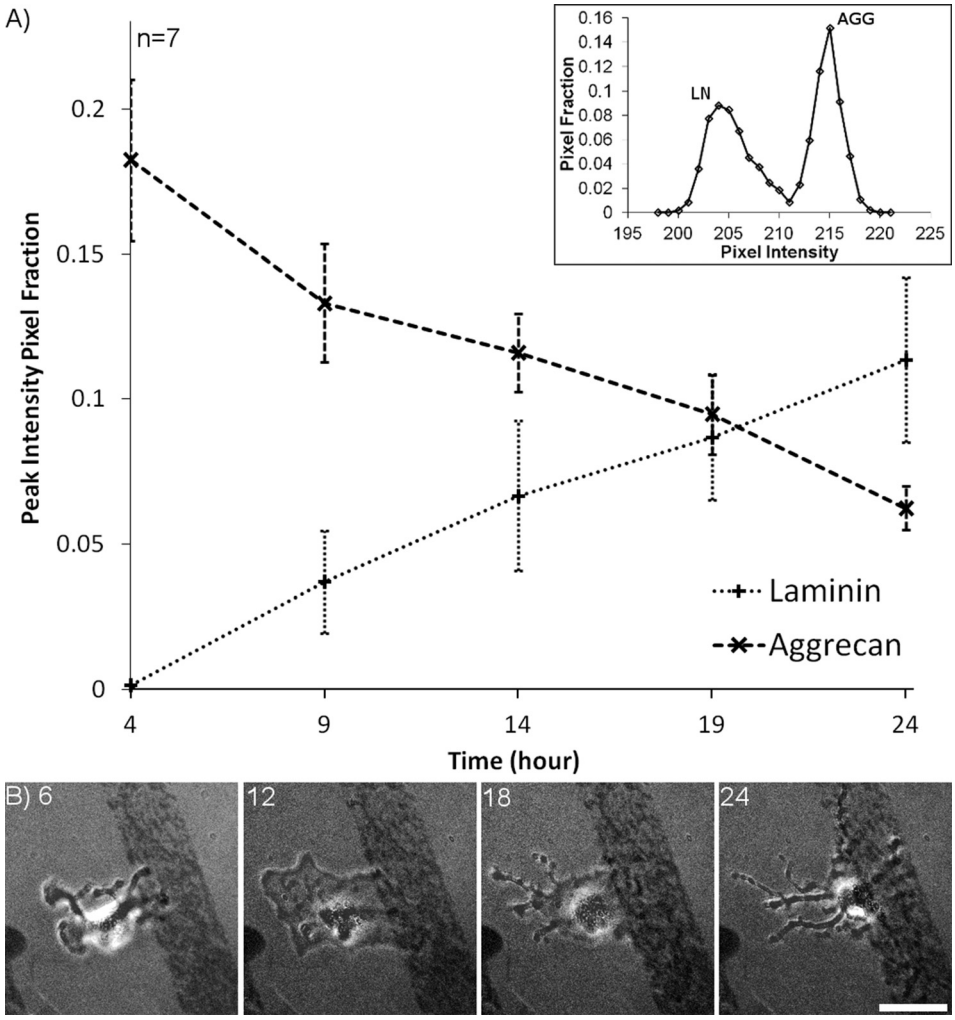

FIG. 5. Astrocyte adhesion footprint shows preference for LN over time. The representative histogram (inset) shows two peaks corresponding to LN and AGG covered by an astrocyte footprint at the 14 h time point. The fraction of pixels of the imaged cell at peak florescence intensities for LN and AGG tracked at 5 h intervals over time. Error bars indicate ±SEM. (b) Astrocyte shifting to gradient pattern 6, 12, 18, and 24 h postseeding. Scale bar = 50 μm.

initially extended process as aforementioned, and astrocytes which encountered both AGG and LN appeared to maintain spreading behavior on LN and not on AGG [Fig. 5(b)]. Previous studies indicated that overall astrocyte adhesion was not influenced by the presence of laminin- or fibronectin-based adhesion peptides compared to plain glass[41] and that substrate stiffness was a larger contributor to astrocyte attachment than LN availability.[42] Therefore, multiple, mixed cues within the cellular span may augment astrocyte extension and sampling of substrate-bound cues compared to binary or uniform substrates (Fig. 4).

Previous studies of the effect that varying stripe widths and spacing's have on confluent layers of astrocytes found that the best astrocyte alignment was achieved with 50 μm-wide stripes of laminin, with 17 μm spacing between them.[43] We previously have effectively aligned multiple layers of astrocytes on 15 μm-wide stripes.[20] Both these widths are well within the range of astrocyte spans found here. Similar values ranging from 100 to 150 μm for the longest astrocyte length have been reported for cultures on poly-L-lysine and silk fibroin fibers.[44] Astrocytes grown on fibronectin-coated polylactic acid fibers for four days were measured to extend processes around 50 μm on random fibers and around 200 μm on aligned fibers,[45] indicating that restricting the available attachment points to the microfibers may extend astrocyte growth even farther than substrate patterns. Therefore, by providing contrasting locations for cellular attachment, astrocytes will extend processes farther. This response could be leveraged to increase astrocyte extension by both modifying substrate geometry and presenting surface-bound permissive and inhibitory molecules.

C. Astrocytes shifted cell bodies onto LN areas, but displacement and speed remained low

Astrocytes preferred to be attached to LN areas over regions of AGG (Fig. 5). In the context of glial scar formation, the upregulation of CSPG expression which is present at the site of CNS injury may impede on astrocyte infiltration into the site. CSPG is known to inhibit supportive Schwann cell migration in the peripheral nervous system.[31] Designing substrates with areas rich in laminin would promote astrocytes to preferentially attach; however, the effect would be

highly localized. Even though astrocytes were capable of moving large distances in the present study, most cells vacillated around a given position where they had initially adhered. The speed of individual cells measured here [Fig. 4(d)] was similar to the speed of 9 μm/h found for populations of astrocytes migrating through cortex *in vivo* and to speeds of mostly 10–20 μm/h for layers of astrocytes closing a scratch wound *in vitro*.[7,13] As previously observed, astrocyte migration to the wound site may not as important as proliferation of the cells bordering the injury for neuroprotective roles.[3] The results from the present study suggest that the idea of covering CNS implant surfaces with astrocytes will likely be analogous to the formation of the glial scar, reliant on astrocyte proliferation at the injury site, as opposed to the recruitment of distant cells. However, the addition of LN patterns to such scaffolds could allow more astrocytes to remain attached to the scaffold and avoid their potential migration away from injury-induced CSPG.

V. CONCLUSIONS

Random dot gradients were created to investigate how astrocytes sample and migrate on surface protein patterns containing mixed adhesion cues. Astrocytes extended processes in a stellate fashion upon initial attachment and maintained extensions as evidenced by increased area and perimeter when presented with AGG but not with LN alone. Astrocytes did not migrate large distances after initial attachment although they shifted their position toward areas with a higher LN/AGG coverage ratio. Cellular extensions were greater when astrocytes interfaced with discrete micrometer-scale patches of LN among those of AGG, spanning a distance of up to 150 μm. These findings indicated that presenting mixed cues on surfaces causes astrocytes to interact with larger areas of the surface, which also allowed astrocytes to preferentially relocate.

ACKNOWLEDGMENTS

This work was supported by NIH Grant Nos. NS057144 and NS088737. The authors would like to thank Brian Baker for assistance in creating stamp templates. The authors also thank M. Condic for valuable discussion and suggestions.

[1]J. R. Faulkner, J. E. Herrmann, M. J. Woo, K. E. Tansey, N. B. Doan, and M. V. Sofroniew, J. Neurosci. **24**, 2143 (2004).
[2]A. Rolls, R. Shechter, and M. Schwartz, Nat. Rev. Neurosci. **10**, 235 (2009).
[3]I. B. Wanner, M. A. Anderson, B. Song, J. Levine, A. Fernandez, Z. Gray-Thompson, Y. Ao, and M. V. Sofroniew, J. Neurosci. **33**, 12870 (2013).
[4]J. Silver and J. H. Miller, Nat. Rev. Neurosci. **5**, 146 (2014).
[5]M. A. Anderson, Y. Ao, and M. V. Sofroniew, Neurosci. Lett. **565**, 23 (2014).
[6]F. Renault-Mihara, S. Okada, S. Shibata, M. Nakamura, Y. Toyama, and H. Okano, Int. J. Biochem. Cell Biol. **40**, 1649 (2008).
[7]H. F. Zhou, L. H.-C. Lee, and R. D. Lund, J. Comput. Neurol. **292**, 320 (1990).
[8]C. Andersson, M. Tytell, and J. Brunso-Bechtold, Int. J. Dev. Neurosci. **11**, 555 (1993).
[9]J. D. Hatton, R. Garcia, and H. Sangu, Glia **5**, 251 (1992).
[10]J. D. Hatton, J. P. Finkelstein, and H. Sangu, Glia **9**, 18 (1993).
[11]S. Bardehle *et al.*, Nat. Neurosci. **16**, 580 (2013).
[12]E. J. Benner *et al.*, Nature **497**, 369 (2013).
[13]Z. Környei, A. Czirók, T. Vicsek, and E. Madarász, J. Neurosci. Res. **61**, 421 (2000).
[14]A. Faber-Elman, A. Solomon, J. A. Abraham, M. Marikovsky, and M. Schwartz, J. Clin. Invest. **97**, 162 (1996).
[15]H. Peng, W. Shah, P. Holland, and S. Carbonetto, Dev. Neurobiol. **68**, 559 (2008).
[16]S. J. A Davies, C.-H. Shih, M. Noble, M. Mayer-Proschel, J. E. Davies, and C. Proschel, PLoS One **6**, e17328 (2011).
[17]S. Han *et al.*, Spinal Cord **52**, 867 (2014).
[18]A. Hurtado, J. M. Cregg, H. B. Wang, D. F. Wendell, M. Oudega, R. J. Gilbert, and J. W. McDonald, Biomaterials **32**, 6068 (2011).
[19]E. East, D. B. de Oliveira, J. P. Golding, and J. B. Phillips, Tissue Eng., Part A **16**, 3173 (2010).
[20]F. Meng, V. Hlady, and P. A. Tresco, Biomaterials **33**, 1323 (2012).
[21]J. K. Alexander, B. Fuss, and R. J. Colello, Neuron Glia Biol. **2**, 93 (2006).
[22]T. W. Hsiao, P. A. Tresco, and V. Hlady, Biomaterials **39**, 124 (2015).
[23]C. L. Lau *et al.*, J. Neurochem. **130**, 215 (2014).
[24]T. Liu, J. D. Houle, J. Xu, B. P. Chan, and S. Y. Chew, Tissue Eng., Part A **18**, 1057 (2012).
[25]R. Fricke, P. D. Zentis, L. T. Rajappa, B. Hofmann, M. Banzet, A. Offenhäusser, and S. H. Meffert, Biomaterials **32**, 2070 (2011).
[26]J. Mai, L. Fok, H. Gao, X. Zhang, and M. Poo, J. Neurosci. **29**, 7450 (2009).
[27]V. J. Tom, M. P. Steinmetz, J. H. Miller, C. M. Doller, and J. Silver, J. Neurosci. **24**, 6531 (2004).
[28]A. C. Von Philipsborn, S. Lang, A. Bernard, J. Loeschinger, C. David, D. Lehnert, M. Bastmeyer, and F. Bonhoeffer, Nat. Protoc. **1**, 1322 (2006).
[29]A. C. Von Philipsborn, S. Lang, J. Loeschinger, A. Bernard, C. David, D. Lehnert, F. Bonhoeffer, and M. Bastmeyer, Development **133**, 2487 (2006).
[30]T. Kuboyama, X. Luo, K. Park, M. G. Blackmore, T. Tojima, C. Tohda, J. L. Bixby, V. P. Lemmon, and H. Kamiguchi, Exp. Neurol. **248**, 157 (2013).
[31]F. T. Afshari, J. C. Kwok, L. White, and J. W. Fawcett, Glia **58**, 857 (2010).
[32]C. D. Eichinger, T. W. Hsiao, and V. Hlady, Langmuir **28**, 2238 (2011).
[33]G. N. Hodgkinson, P. A. Tresco, and V. Hlady, Biomaterials **33**, 4288 (2012).
[34]G. N. Hodgkinson, P. A. Tresco, and V. Hlady, Biomaterials **29**, 4227 (2008).
[35]K. D. McCarthy and J. de Vellis, J. Cell Biol. **85**, 890 (1980).
[36]J. E. Bottenstein and G. H. Sato, Proc. Natl. Acad. Sci. **76**, 514 (1979).
[37]T. W. Hsiao, V. Swarup, and C. D. Eichinger, "Glycosaminoglycans," in *Methods in Molecular Biology*, edited by V. Hlady, K. Balagurunathan, H. Nakato, and U. R. Desai (Springer, New York, 2015), pp. 457–467.
[38]R. Delgado-Gonzalo and M. Unser, IRBM **34**, 235 (2013).
[39]A. F. Levy, M. Zayats, H. Guerrero-Cazares, A. Quiñones-Hinojosa, and P. C. Searson, PloS One **9**, e92165 (2014).
[40]A. L. Placone, P. M. McGuiggan, D. E. Bergles, H. Guerrero-Cazares, A. Quiñones-Hinojosa, and P. C. Searson, Biomaterials **42**, 134 (2015).
[41]L. Kam, W. Shain, J. N. Turner, and R. Bizios, Biomaterials **23**, 511 (2002).
[42]P. C. Georges, W. J. Miller, D. F. Meaney, E. S. Sawyer, and P. A. Janmey, Biophys. J. **90**, 3012 (2006).
[43]C. Kofron and D. Hoffman-Kim, Cell. Mol. Bioeng. **2**, 554 (2009).
[44]J. Qu, D. Wang, H. Wang, Y. Dong, F. Zhang, B. Zuo, and H. Zhang, J. Biomed. Mater. Res., A **101**, 2667 (2013).
[45]J. M. Zuidema, M. C. Hyzinski-García, K. Van Vlasselaer, N. W. Zaccor, G. E. Plopper, A. A. Mongin, and R. J. Gilbert, Biomaterials **35**, 1439 (2014).